

RFQ Cooler SHIRaC for SPIRAL 2: Cooling of very high intensity beam

Ramzi.Boussaid^a, G.Ban^a, A.Rebai^b

^aLPC-IN2P3-CNRS, ENSICAEN, 6 Boul. Maréchal Juin, 14050 Caen, France.

^bSUBATECH IN2P3-CNRS/Université de Nantes/Ecole des Mines de Nantes, Nantes, France

Abstract:

The experimental study of Spiral-2 High Intensity Radiofrequency Cooler prototype is presented. The handling of beam's intensity going up to 1 μ A is the mainly adding of this work. The development of the design, the vacuum system and the RF system is outlined. The experimental results in terms of transmission, geometrical emittance, longitudinal spread energy and purity of cooled beams will be discussed. The reduction of the longitudinal spread energy degradation, induced by the derivative of the RF voltage at the RFQ exit, in adding a miniature RFQ Cooler will be studied via numerical simulations. The coupling between the RFQ Cooler and the high resolution separator by an electrostatic triplet will be examined.

Keywords: buffer gas cooling, RF system, vacuum system, diagnostic beam, Space Charge, buffer gas diffusion, derivative of the RF voltage.

Introduction

The next low energy DESIR/SPIRAL2 facility is a second generation installation of high intensity radioactive ions beams [1]. Such beams will require an isobaric purification of isotopes. A highest resolution magnetic separator (HRS) coupled to a buffer gas RF cooler can achieve this purification level. The HRS was developed at CENBG laboratory [2]. Although, The RF Cooler commonly called SHIRaC, Spiral 2 High Intensity Radioactive Cooler, is developed and tested in LPC Caen (France)[14][15]. The nominal working of HRS requires the followings specifications of RFQ Cooler: an emittance $\varepsilon < 3 \pi$.mm.mrad, a longitudinal spread energy $\Delta E \approx 1$ eV and transmission at least 60 % for ion's mass $m > 90$ u.m.a, more than 40 % for $m > 60$ u.m.a and more than 20 % for $m > 20$ u.m.a.

The mainly specificity of this Cooler is the handling of very high intensity beam going to 1 μ A, so more than the existant intensity beam by two or three magnitude order, where the space charge effect become very significant. To reduce this effect, high RF voltage amplitude and high frequency, few kV and few MHz, must be used. The latter characteristics are what distinguish this Cooler from those who are existing.

In this paper we will present the RF system, the vacuum system and the diagnostics beams. We will also present the experimental results of cooling in terms of the transmission efficiency, the longitudinal spread energy, the transversal emittance and the purity. We will also discuss the effects of the space charge, the buffer gas diffusion and the RF voltage on the cooled beam properties. We will advise, via numerical simulations, a solution to reduce the degradation of the cooled beams.

At the ending, we will study the coupling between the RFQ Cooler and the HRS by an electrostatic triplet.

1. Experimental setup

1.1 RFQ Cooler beam line

The RFQ Cooler prototype consists mainly of three sections: the injection and deceleration section, the RFQ chamber and the extraction and reacceleration section (Figure 1). The details dimensions of sections are presented in reference [14][15].

The injection section consists of a deceleration system and an electrostatic lens. It allows a deceleration of ions coming from the source to about 100 eV.

The RFQ is placed in a chamber filled by a buffer gas and set to the high voltage. To adapt to SPIRAL2/DESIR authentic beams, the internal radius was $r_0=5$ mm [7]. The RFQ is segmented to 18 equidistant segments of 40 mm of length.

The extraction cell is placed at the outlet of the RFQ. It consists of three cylindrical electrodes with different size and openings. Its goal is to accelerate the ions to their initial energy.

1.2 RF system

The confinement of ions is achieved by applying RF voltages on the quadrupole electrodes. In our case, the strongest RF amplitude and correspondingly highest frequencies should be used [16,17,18]. Thus, RF parameters are of few kV and few MHz [14,19,20]. The existing Coolers are working for about few hundred volts at one MHz [19].

The RF system is a critical part of the instrument because the electric breakdown [16] and the ceramic insulator burning can occur from a few kV of RF amplitude. To avoid the burning the whole internal structure is done by the PEEK (Figure 3). In order to achieve high voltages amplitude without breakdown, the RF system being a resonant LC circuit (Figure 5); two hollow coils and a parallel air induction system. This system lets us to reach 10 kV

of RF voltages amplitude and frequencies not exceeding 8 MHz without being limited by any breakdown problem. In order, to handle the widest range of masses, the capacity being chosen variable (figure 5).

1.3 Vacuum system

The cooling beam is provided by the successive collisions ions-buffer gas into the RFQ chamber. Its optimum can be done for a gas pressure of few Pa [3]. As the RFQ chamber is in physical contact with the other sections, the buffer gas diffusion can be done. To reduce this diffusion, the injection and the extraction plates sizes have been

choose as small as possible, with dimensions of 6 and 4 mm respectively, and a differential pumping system of high capacity was installed, see figure 3. This system consists of two turbo molecular pumps of capacity 300 l/s on either side of RFQ chamber and two turbo molecular pumps of capacity 1000 l/s on the source and after extraction section [7].

In Figure 3 we present the measurements of the pressures distributions along the experimental line with different RFQ pressure. We note that in the outside of RFQ chamber the pressure does not exceed 1/100 RFQ pressure.

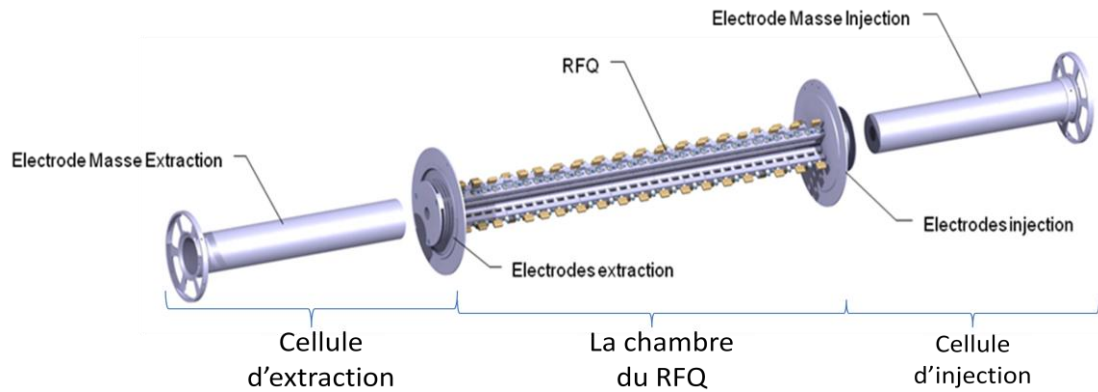


Figure 1: three cells of experimental setup RFQ Cooler SHIRaC

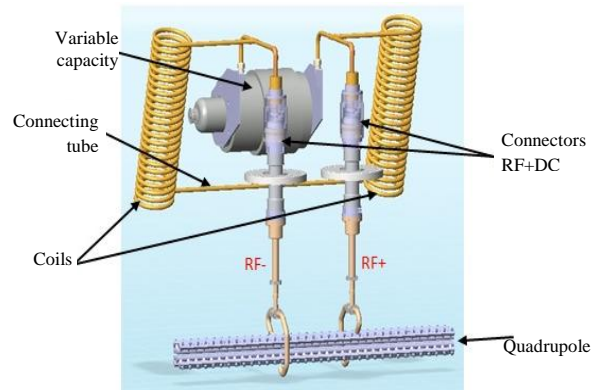
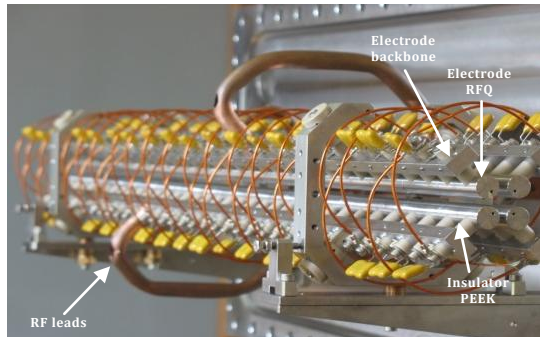


Figure 2: The design of the RFQ and the voltages delivery scheme to the quadrupole electrodes.

20	1,31E-05	5,36E-05	2,08E-02	1,22E-04	2,28E-05
25	1,65E-05	6,70E-05	2,58E-02	1,68E-04	2,90E-05
30	2,00E-05	9,12E-05	3,05E-02	2,10E-04	3,52E-05
Débit ml/min	P cible (mBar)	P extraction (mBar)	Pression RFQ (mBar)	P injection (mBar)	P Source (mBar)

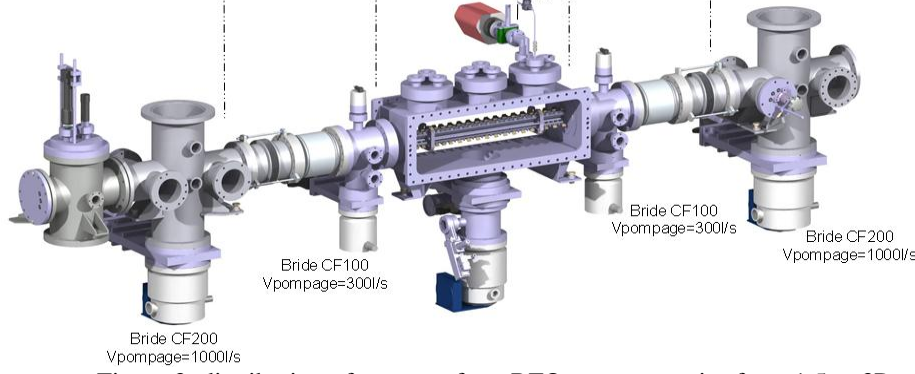


Figure 3: distribution of pressure for a RFQ pressure varies from 1.5 to 3Pa.

2. Experimental studies

We will present the cooling experimental results of heavy mass cesium $^{133}\text{Cs}^+$ ions beam delivered by an ionization surface source IGS4 of energy 5 keV and of emittance around $10 \pi \cdot \text{mm} \cdot \text{mrad}$. We will focus on the effects of the space charge, the RF voltage and the buffer gas pressure on the transmission, the geometrical emittance ϵ , the longitudinal spread energy ΔE and the cooled beam purity.

Firstly, we define the optimum running parameters in terms of the RFQ pressure and the guiding field.

2.1. Running parameters

The RFQ pressure and the guiding field are the running parameters which correspond to the optimum cooling with the maximum of transmission. From figure 5 we observe that the transmission increases with pressure until a maximum of 66% at for 2.5 Pa before declining. The decrease is explained by the stop of ions in the RFQ after the multiple collisions.

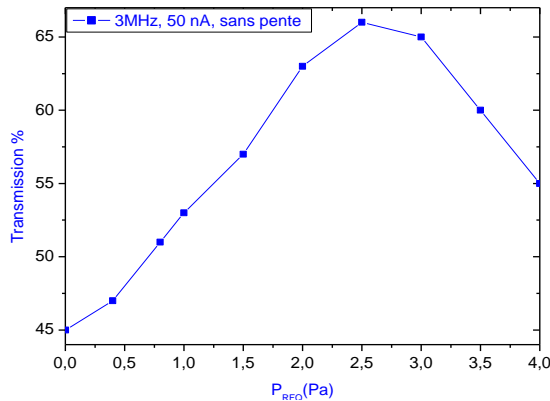


Figure 4: Variation of transmission with RFQ pressure PRFQ.

To counter the ions stopping into the RFQ and to improve the transmission a DC guiding field of ions must be added. Therefore, the transmission is improved and it passes by a maximum for a guiding

field of 16 V/m (Figure 6). The transmission behavior is explained by the competition between the cooling effect due to the gas pressure in the RFQ and the accelerator effect of the guiding field. The reached values for the transmission reflect this competition and a maximum of 74% reached.

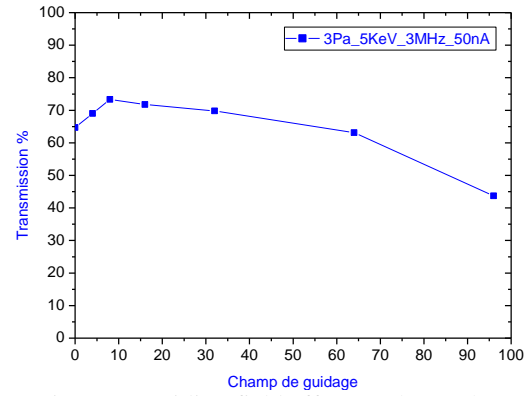


Figure 5: Guiding field effect on the on the transmission.

In conclusion, the optimum cooling is obtained with an RFQ pressure around 2.5 Pa and a DC guiding field of 16 V/m.

2.2. Transmission measurements

We will study the dependencies of the transmission to the space charge and the RF voltage.

Transmission measurements are determined as the ratio of current beam after the extraction section by the one at the injection section, measured by a cup Faraday.

Space charge effect

As presented in references [14,15], the lost of ions during the cooling and mainly at the RFQ exit is due to the space charge effect. With the below figure we will deal quantitatively these lost. At very low intensity, less than 200 nA, where the space charge effect is negligible more than 90 % of ions can reach the extraction region and less than 10 % of ions are lost during the injection. Beyond this current beam

region, the transmission decreases quickly to 68 % at 1 μ A.

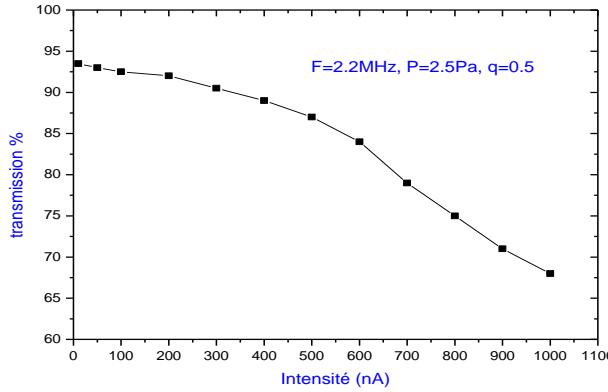


Figure 6: Space charge effect: transmission versus of the current beam for a RFQ pressure of 2.5 Pa

RF voltage effect

The dependence of the transmission to Mathieu parameter q i.e. to the RF voltage is communally called the stability diagram. At high intensity, a widening phenomenon of this diagram can be occurred [8]. Using the below figure we attempt to study this widening. The transmission increases from zero for $q=0$ until a maximum reached for q between 0.3 and 0.6. Beyond $q>0.6$, it decreases and reaches 0 for $q=0.9$. Therefore, none widening phenomenon is observed at 1 μ A. From this diagram we confirm another time that the optimum cooling is obtained with an RFQ pressure of 2.5 Pa because the transmission with this pressure is better than one with 3 Pa.

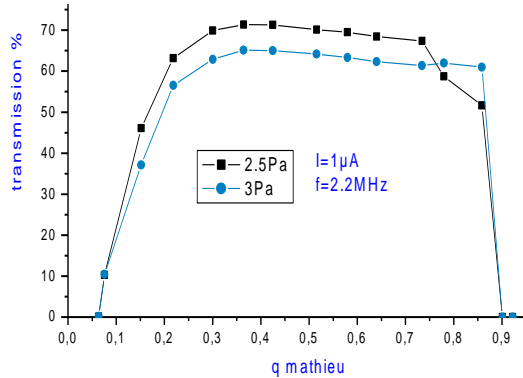


Figure 7: Stability diagram at 1 μ amps for frequency of 2.2 MHz

2.3. Geometrical emittance

The emittance measurement was done by a Pepperpot emittance meter and we will present its equivalent for an energy of 60 keV. Figure 10 shows the dependence of these measurements to the RF voltage and the space charge. The effect of the RF voltage on the cooling is clear when the emittance decreases slowly with q and in the absence of space charge effect, low than 100 nA, it is around 1 π .mm.mrad for $q>0.15$. When the current beam

increases the emittance also increases and for 1 μ A it is less than 2 π .mm.mrad for $q>0.15$.

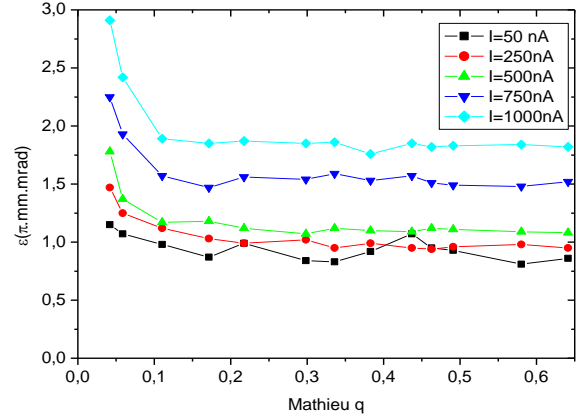


Figure 8: Variation of emittance with parameter q at different intensities

2.4. Longitudinal spread energy

To determine this parameter we measure the variation of the transmission as a function of the last RFQ electrode DC voltage. The FWHM (full width at half maximum) of the derivative of this variation is defined as the longitudinal spread energy ΔE .

Space charge effect

The simulations results presented in reference [15] have shown that the space charge effect have an important contribution in the degradation of the longitudinal spread energy. The below figure shows quantitatively this contribution for currents beam going up to 1 μ A. This degradation with the current beam is clear when the current beam increases and even at low intensity (<100 nA) the spread energy is very far to 1 eV. To explain this behavior at low intensity we must study the effect of the RF voltage on the spread energy.

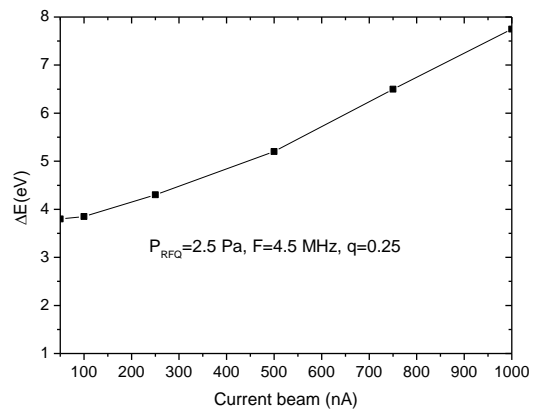


Figure 9: Space charge effect on the longitudinal spread energy

RF voltage effect

The dependence of ΔE to the RF voltage V_{RF} will be discussed in this part. As the V_{RF} and the Mathieu parameter q are proportional it is commode to study the variation of the transmission with the q parameter. In Figure 11 we present the variation of ΔE

and its corresponding transmission as a function of q for current beam of $1 \mu\text{A}$. Contrary to the behavior of the cooled beam with the V_{RF} which is the diminution of ΔE with the V_{RF} , here we note that ΔE increases with q so with the V_{RF} . This increase doesn't explain the effect of the V_{RF} on the cooling i.e. on the ΔE but it explains the degradations of the cooled beam by the RF voltage at the RFQ exit region where the transversal RF field, created by the RF quadrupole, induces a RF longitudinal field. This longitudinal field degrades the longitudinal velocities distribution of cooled ions via its randomly characteristic. This randomly characteristic result from the temporal dependence of the RF voltage. In spite of these degradations a minimum of ΔE is obtained for 1 kV of RF voltage and it is due to a competition between the cooling effect of the RF voltage and the longitudinal RF field. At this minimum the ΔE is around 3.7 eV for a transmission of 53 %. For a transmission at least 60 % the longitudinal spread energy is around 5 eV.

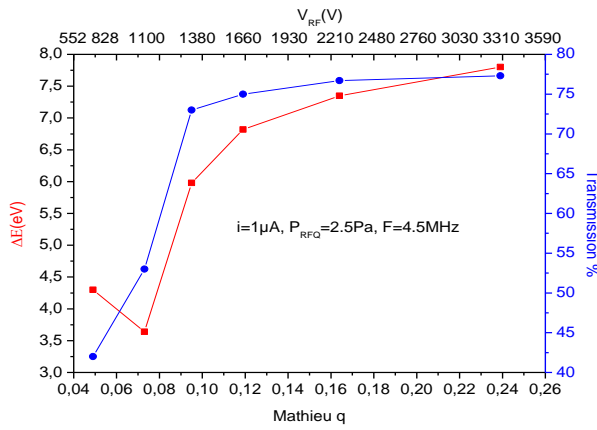


Figure 10: Variation of the transmission and ΔE as a function of parameter q

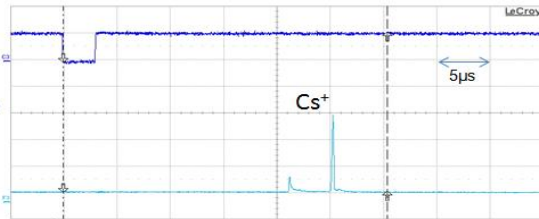
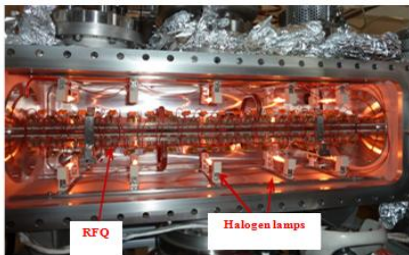


Figure 12: Stoving technical into the RFQ chamber (left) cooled ions spectrum after the stoving of the RFQ chamber

3. Coupling RFQ–HRS: electrostatic triplet

The cooled ions beam going to HRS should pass through a rectangular slit of $1 \times 4 \text{ mm}^2$ of dimension placed at the inlet of HRS. Without any ion optical device less than 20 % of these ions can reach the HRS. In order to avoid these losses, an ion optical device must be setup between the RFQ Cooler and the HRS. This device must be running with only few kV for energy beams going up to 60 keV. The only way is a multiple electrostatic quadrupole, a triplet of quadrupole. Each quadrupole provide a convergence in one transversal direction and a divergence in the

2.6 Purity of cooled beams

The ions being very slow in the RFQ chamber, chemical reactions on the residual gas may occur. From the spectrum of figure 21, we observe the presence of impurities of H_2O , CO_2 , N_2 ... which their weight does not exceed 55 u.m.a [10] while we would not expect to observe that Cs ions. Nevertheless, we don't see molecules formed with Cs ions. We note that the presence of peaks meets the stability condition imposed by the Mathieu parameter q , figure 21. Beyond the stability region of each ions type it will be trapped into the RFQ chamber. An electronic peak is observed at 21 μs .

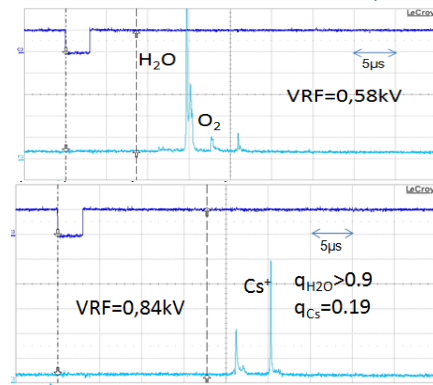


Figure 11: cooled ions mass Spectrum with different RF voltages and for $I=50 \text{ nAmps}$, $P_{\text{RFQ}}=2.5\text{Pa}$, $F=2.5\text{MHz}$.

To remove the impurities observed in the above mass spectrum, we applied the stoving technical. This technical consists stove the internal RFQ chamber with halogen lamps, figure 22. After the stoving, a pure spectrum with only Cs ions peak at different RF voltage is obtained, see figure 23.

other one transversal direction. The optimization of its dimensions is doing by Simion 3D V8.1 and they are presented on the followings figure 13: EQ 80 mm-drift 60 mm-EQ 160 mm-drift 60 mm-EQ 80 mm, where EQ stands for electrostatic quadrupole. In order to avoid the edge effect, cylindrical discs are put on either side of each quadrupole.

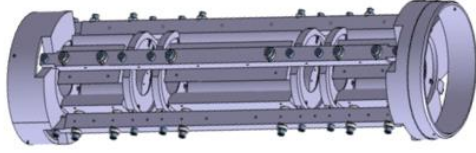


Figure 13: Schematic design of electrostatic triplet

In the below figure we have the measurement of the cooled ions beam profiles along two transversal directions and for different current beam. These profiles are fitted as a Gaussian curve. The FWHM of these curve at the different current beam is presented

in the below table. For current beam going up to 1 μ A more than 95% of ions passes through the slit.

Intensity (nA)	σ_x (mm)	σ_y (mm)
50	0.231	0.347
250	0.246	0.350
500	0.242	0.362
750	0.308	0.579
1000	0.374	0.586

Table 1: Transversal sizes FWHM of the cooled ions beam profile for different current beam.

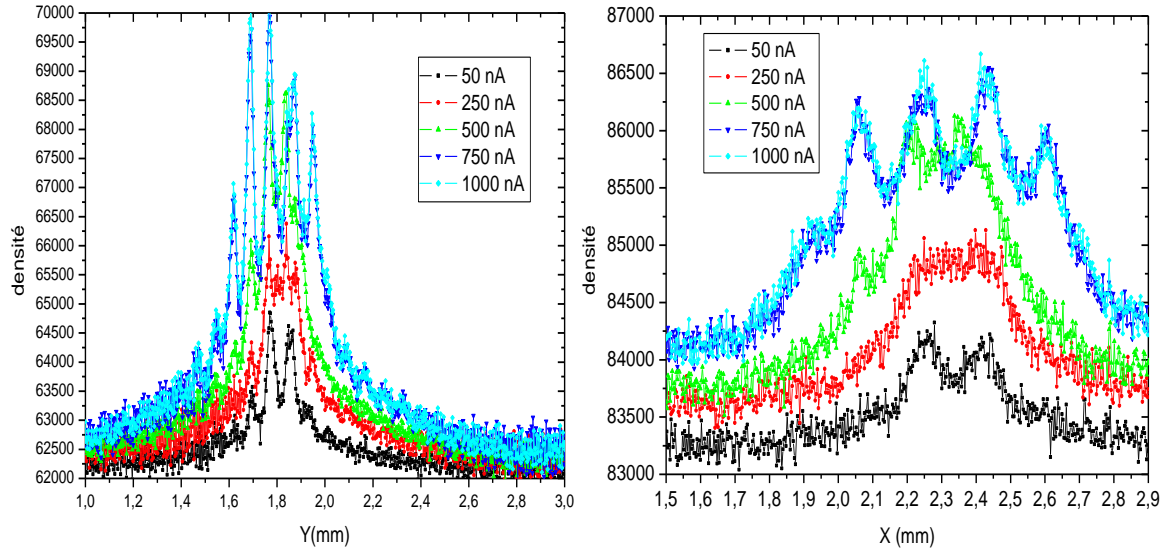


Figure 14: Cooled ions beam transversal profiles after the triplet for different current beam: along the convergent transversal direction (left) and along the divergent transversal direction (right).

4. Miniature RFQ Cooler

To reduce the longitudinal spread energy degradation with the RF voltage we set up a miniature RFQ at the RFQ exit. This device can contribute to reduce the buffer gas diffusion and the space charge effects which can occur at the RFQ exit [14,15]. The optimization of its dimensions is done by the Simion 3D V8.0. These dimensions are 40 mm of length and 2 mm of inner radius. In order to reduce to maximum possible the buffer gas diffusion, the miniature RFQ electrodes are half circular. With this device, the pressure distribution along the RFQ cooler beam line is kept.

To avoid the creation of any longitudinal RF field between these two RFQ and any acceleration or deceleration of ions in this region, the miniature RFQ must run with the same frequency of the RFQ and with a reduced RF voltage amplitude. From figure 10 we can deduce that the longitudinal RF field effect is negligible for RF voltage amplitude less than 1 kV. That is why, the miniature RFQ is alimented by an RF voltage amplitude of 441 V for 4.5 MHz of frequency, so $q=0.4$.

The simulations of the cooling and the transport of the cooled ions beam is based on the Simion 3D program and the hard disc model presented

in reference [14,15]. We used a $^{133}\text{Cs}^+$ ions beam of 60 keV of energy and of 80 π .mm.mrad of emittance.

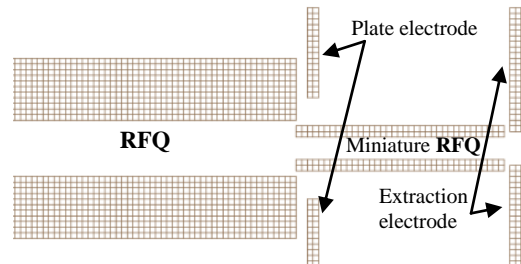


Figure 15: positioning of the miniature RFQ and layout of the new extraction section

RF voltage effect

The below figure illustrate the simulated results of the longitudinal spread energy as a function of RF voltage, the q parameter. The longitudinal RF field effect is deleted because the longitudinal spread energy doesn't increase with the RF voltage but rather it decreases with the RF voltage and become stable for q between 0.3 and 0.5. This behavior of ΔE explains very well the RF voltage effect on the cooling into the RFQ. Beyond this region of q the ΔE increases because the RF heating is important.

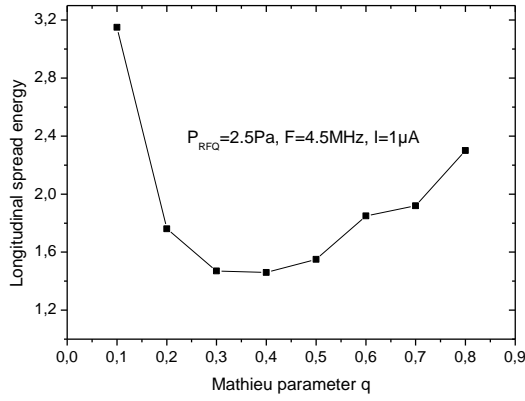


Figure 16: RF voltage effect on the longitudinal spread energy for 1μA.

Space charge effect

The contribution of miniature RFQ in the reduction of the space charge effect exit is noticeable because it allows the transport of the cooled ions from the RFQ exit where their kinetic energy is around only few eV to this limit where their energy is around 30 eV and then to a region where the space charge effect is low. The below figure illustrate this contribution. As we can see, the ΔE increases progressively with the current beam from 1.1 eV to 1.4 eV for current beam going from 50 nA to 1 μA. The reduction of the space charge effect is manifested in the reduction of the variation gap of the ΔE , for current beam going from

50 nA to 1 μA, from 4 eV (see figure 9) to only 0.3 eV.

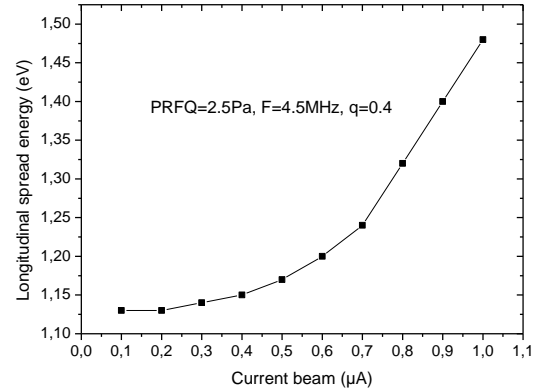


Figure 17: Space charge effect on the longitudinal spread energy for q=0.4

Before to conclude, we present the new properties of 1μA cooled ions beam in terms of the geometrical emittance ε which can be define as an ellipse containing 95% of these ions, then:

$$\varepsilon = 4\sigma_{\theta X} * \sigma_X$$

From the below figure, the Gaussian fit of the elevation angle θ_x and the radial distribution x take an emittance around $1.84 \pi \cdot \text{mm} \cdot \text{mrad}$.

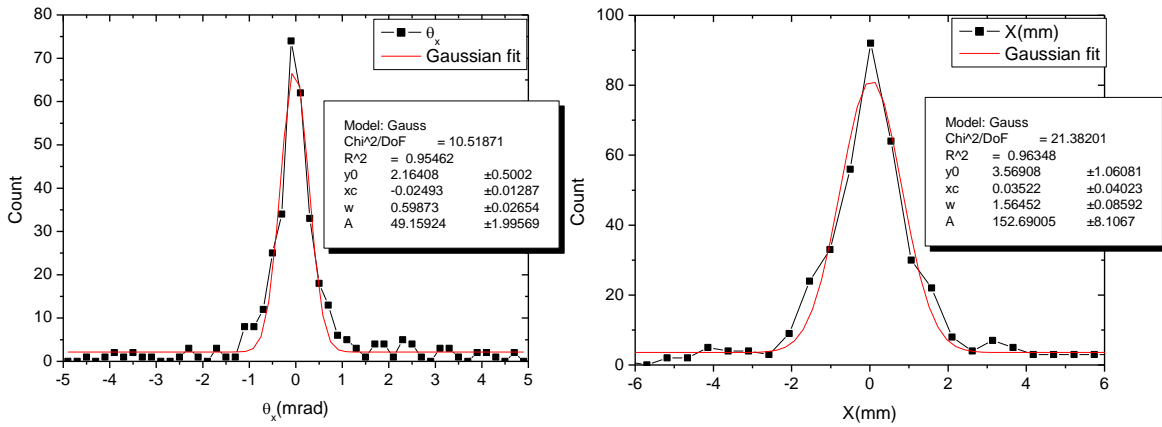


Figure 18: characteristics of 1μA cooled ions beam: distributions of the elevation angle θX (left) and the distributions of the radial position X(right).

Conclusion

Theoretically, the disadvantage of high intensities ions beams cooling was the space charge but the present experimental studies allow us to note that the derivative of the high RF amplitude can occur at the RFQ exit a longitudinal RF field which can be more relevant than the first one. The first one is responsible to the degradation of the transmission and the emittance however the second degrades the longitudinal spread energy.

To reduce their effect, a miniature RFQ is installed at the RFQ exit. It allows us to avoid the degradation of the cooled ions by these effects and to guide these ions to a region where their energy is more

than 30 eV and then they can resist to any degrading effects.

In front of the HRS, the 1μA cooled ions beam has an emittance of $1.8 \pi \cdot \text{mm} \cdot \text{mrad}$, a transmission around 70 % and a longitudinal spread energy of 1.4 eV. Therefore, an isobaric purification of this cooled ions beam by the HRS will become possible.

References:

- [1] M.Lewitowicz, Nucl. Phys. A 805 (2008) 519-525c, GANIL.
- [2] M.Lewitowicz, ACTA Physica Polonica B, Vol 42(2011)
- [3] T.Kim. PhD thesis, McGill university, 1997.

- [4]S.Henry, PhD thesis, univ Louis Pasteur, 2001.
- [5]I.Podadera, et Al., Nuclear Physics A 746: 647–650(2004).
- [6]D.Lunney et al. Journal of Modern Optics, 39:349, 1992.
- [7]F.Duval, PhD thesis. Caen Basse Normandie Univ 2009.
- [8]D.J.Douglas et al.. Mass spectrometry Rev, 2005, 24, 1-29.
- [9]S.Jolly. proceeding of DIPAC09, basel, Switzerland.WEA 03.
- [10] S.Heinz et al., Nucl. Instrum.And. Meth. A 533. 239-247. (2004).
- [11]Hoffman.Edmont,Vincent Stroobant. Toronto: John Wiley & Sons, Ltd. P.65. ISBN 0-471-48566-7. (2003).
- [12]R.B.Moore, 1998, private communication.
- [13]Yost,R.A;C.G. J.A Chemical Society 100(7):2274.Doi:10.1021/ja00475a072.(1978).
- [14]R.Boussaid et Al, al., Nucl. Instrum.And. Meth. A (2014).
- [15]R.Boussaid, PhD thesis. Caen Basse normandie university (2012).
- [16]S.Schwarz. Nucl. Instr. And Meth, A 566 (2006) 233-243.
- [17]Ghosh, P.K.: Ion Traps, 22. Oxford Science, Oxford, UK (1995).
- [18]C.Bachelet et Al, Hyperfine interact (2006) 173:195-200.
- [19] O. Gianfrancesco et al., Nucl. Instr. and Meth. in Phys. Res. B 266 (2008) 4483–4487
- [20]R.B.Moore, O.Gianfrancesco,. N.I. and .M. in physics research B 204 (2003) 557-562.